

# Lawrence Berkeley National Laboratory

## Recent Work

**Title**

K VACANCY PRODUCTION BY 4.88 GeV PROTONS

**Permalink**

<https://escholarship.org/uc/item/1wv035kq>

**Author**

Anholt, R.

**Publication Date**

1976-04-01

0 0 0 4 4 0 3 2 3 4

Submitted to Physical Review A

LBL-4307 Rev.  
Preprint c.1

K VACANCY PRODUCTION BY 4.88 GeV PROTONS

R. Anholt, S. Nagamiya, J. O. Rasmussen, H. Bowman,  
J. G. Ioannou-Yannou, and E. Rauscher

April 1976

RECEIVED  
LAWRENCE  
BERKELEY LABORATORY

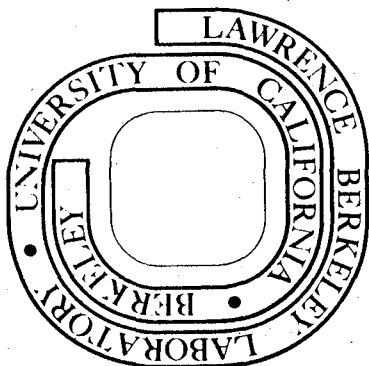
AUG 3 1976

LIBRARY AND  
DOCUMENTS SECTION

Prepared for the U. S. Energy Research and  
Development Administration under Contract W-7405-ENG-48

**For Reference**

Not to be taken from this room



LBL-4307 Rev.  
c.1

## **DISCLAIMER**

This document was prepared as an account of work sponsored by the United States Government. While this document is believed to contain correct information, neither the United States Government nor any agency thereof, nor the Regents of the University of California, nor any of their employees, makes any warranty, express or implied, or assumes any legal responsibility for the accuracy, completeness, or usefulness of any information, apparatus, product, or process disclosed, or represents that its use would not infringe privately owned rights. Reference herein to any specific commercial product, process, or service by its trade name, trademark, manufacturer, or otherwise, does not necessarily constitute or imply its endorsement, recommendation, or favoring by the United States Government or any agency thereof, or the Regents of the University of California. The views and opinions of authors expressed herein do not necessarily state or reflect those of the United States Government or any agency thereof or the Regents of the University of California.

## K VACANCY PRODUCTION BY 4.88 GeV PROTONS

R. Anholt,\* S. Nagamiya, J. O. Rasmussen, H. Bowman,  
J. G. Ioannou-Yannou and E. Rauscher

Lawrence Berkeley Laboratory  
University of California  
Berkeley, California 94720

April 1976

## ABSTRACT

Cross sections for K vacancy production by 4.88 GeV protons on elements between Ni and U have been measured. These cross sections lie approximately a factor of two above the Binary Encounter and Plane Wave Born Approximation predictions. To partially explain these deviations, we argue that an additional contribution due to the interaction between the currents of the projectile and target electron must be added these theories.

## I. INTRODUCTION

In recent years much effort has been devoted to measuring cross sections for K vacancy production by energetic protons and alpha particles in medium heavy and heavy elements.<sup>1</sup> Most of this work has been done at energies between a hundred keV and 30 MeV per nucleon. Three theories exist that predict the cross sections: the Binary Encounter Approximation (BEA),<sup>2,3</sup> the Plane Wave Born Approximation (PWBA),<sup>4</sup> and the Semiclassical Approximation (SCA).<sup>5</sup> To first order, these theories predict that the K vacancy cross sections should fit on a universal curve and should be a function only of the K shell binding energy  $U_K$ , the atomic number of the projectile  $Z_1$ , and the ratio of the projectile velocity to the velocity of the electron in the K shell  $v_1/v_K$ . Nearly all of the data taken fits the universal curve to within approximately a factor of two.

K vacancy production by very relativistic protons has not yet been examined.<sup>1</sup> Non-relativistically, the cross sections depend on just the ratio  $v_1/v_K$  and hence one can actually examine the high energy part of the universal curves by measuring K vacancy production cross sections by moderately energetic protons on very light elements. Thus far, though, these non-relativistic measurements<sup>6</sup> have not exceeded  $v_1/v_K \approx 2.16$ . With 4.88 GeV protons, it is possible to obtain  $v_1/v_K \approx 5$  (on Ni) which is much larger than any previous measurement. In addition to the large  $v_1/v_K$ , however, there is the possibility that additional relativistic effects on the cross sections may be investigated. Previously the highest energy work has been done with 160 MeV

protons,<sup>7</sup> where no dramatic deviation from the nonrelativistic PWBA theory was found. The cross sections simply decreased roughly as the inverse square of  $v_1/v_K$ , as predicted by the PWBA and BEA theories. The authors of that work compared their results with relativistically calculated cross sections for K vacancy production by incident electrons, suggesting that at proton energies slightly higher than 160 MeV, relativistic effects may cause the cross section to rise again.

We originally undertook this work in order to test whether such a rise in the cross section may be observed at 4.88 GeV. In Section II of this paper we present our experimental work and final cross sections, which are higher than the BEA and PWBA theory predictions. To partially explain these deviations we show that an additional term must be added to the BEA or PWBA section.

While those theories adequately account for the interaction between the static Coulomb fields of the projectile and target electrons, they neglect the additional interaction between the currents of the two charged particles.<sup>8-11</sup> This current-current interaction should be important in this case since the projectile current has  $\beta \approx 1$ . In almost all data previously taken,  $\beta$  was small; hence, that contribution could be neglected. The K vacancy cross sections are calculated in Section III and are compared with experimental results in Section IV.

## II. EXPERIMENT

The experimental configuration is schematically illustrated in Fig. 1. Protons of 4.88 GeV from the Lawrence Berkeley Laboratory Bevatron passed through a 0.0254-mm Ag monitor foil, a 0.00608 to

0.0508 mm target foil, a scintillation paddle, an ion chamber, and a TV monitor paddle with negligible energy loss. A horizontally placed Si(Li) detector viewed the target at right angles to the beam, and a Ge(Li) planar detector, facing upward, likewise viewed the target at right angles to the beam. The target was tilted vertically by  $45^\circ$  and was rotated by  $45^\circ$  so that its normal was  $60^\circ$  to the beam and its plane face was  $45^\circ$  from both the Si(Li) and Ge(Li) detectors. Both detectors also viewed the Ag monitor foil, which was placed 10 cm upstream from the target. To make deadtime corrections, pulses from each detector fired a fast discriminator which supplied one pulse every hundred pulses to trigger a pulser on the opposite detector. The number of pulses triggered ( $p_{in}$ ) was recorded and later the number of pulses counted ( $p_c$ ) was found. The deadtime correction ( $p_{in}/p_c - 1$ ) varied between 0.4% and 50%.

To monitor the beam intensity we relied on an ion chamber coupled to an electrometer and integrator to integrate the relative intensity of the beam from run to run. The absolute intensity of the beam was found by irradiating a 0.95-cm-thick graphite target and then we off-line counted the annihilation radiation from the  $\beta^+$  decay of  $^{11}\text{C}$  formed in the  $^{12}\text{C}(p,pn)^{11}\text{C}$  reaction. Since the  $^{11}\text{C}$  reaction has a known (interpolated) cross section for 4.88-GeV protons,  $28 \pm 0.6 \text{ mb}$ ,<sup>12,13</sup> the absolute number of protons passing through the carbon target and ion chamber could be found. Seven calibration runs were taken. The measured number of particles per ion chamber reading varied by less than 2%.

To obtain cross sections insensitive to the uncertainty in the detector deadtime, we measured all of the x-ray yields relative to the yield of Ag K $\alpha$  x-rays observed in the monitor foil which, together with the detectors, remained in a fixed position throughout the entire experiment. For some 40 runs we averaged the quantity

$$x = \frac{C(\text{AgK}\alpha)}{\text{I.C.}} \frac{P_{\text{in}}}{P_c}, \quad (1)$$

where  $C(\text{AgK}\alpha)$  is the counts observed in the monitor foil, I.C. is the ion chamber reading, and  $p_{\text{in}}/p_c$  is the pulser-measured deadtime correction. The yield for an x-ray of energy  $E_x$  was found by:

$$Y = \frac{C(E_x)}{C(\text{AgK}\alpha)} \frac{\langle x \rangle A}{F(E_x)P} \text{ photons/proton}, \quad (2)$$

where  $P$  is the number of protons per ion chamber reading,  $F(E_x)$  is the detector efficiency,  $C(E_x)$  is the counts observed in the x-ray peak of energy  $E_x$ , and  $A$  is the correction for air and Be attenuator absorption.

To obtain cross sections, this yield was divided by the target atom density and effective thickness  $[1 - \exp(-\mu t)]/\mu$ , where  $t$  is the thickness of the tilted target and  $\mu(E_x)$  is the attenuation coefficient of the target fluorescent x-rays in the target material.<sup>14</sup> The cross sections for the K $\alpha$  and K $\beta$  peaks (where separable) were then added, and the neutral atom fluorescent yield<sup>15</sup> was used to convert the x-ray cross sections to vacancy cross sections.

The uncertainties in these procedures were as follows:

- (1) Protons per ion chamber reading (counting statistics, <sup>11</sup>C cross section,  $\beta^+$  counter efficiency, graphite



-5-

- target thickness):  $\pm 4\%$
- (2) Detector efficiency:  $\pm 8\%$  Si(Li),  $\pm 14\%$  Ge (Li)
  - (3) Average number of deadtime corrected Ag K $\alpha$  counts per ion chamber reading ( $\langle x \rangle$ ):  $\pm 13\%$  Ge(Li),  $\pm 7\%$  Si(Li)
  - (4) Target angle, thickness, absorption coefficient:  $\pm 2\%$
  - (5) Counting statistics, including variation from run to run:  $\pm 2 - 10\%$ .

In addition, one other correction for target thickness needs to be made. Plots of the cross sections as a function of target thickness (Fig. 2) show that there is a definite trend for the observed cross sections to increase with target thickness. This is due mainly to two secondary processes:<sup>7</sup> (1) protons making energetic secondary electrons in the target which excite K vacancies, and (2) protons making secondary electrons which emit bremsstrahlung radiation in collisions with other target nuclei, which photoelectrically excites K vacancies. For thin targets the former process increases the cross section linearly with target thickness; the latter process increases it quadratically.

To adjust our measured cross sections to zero target thickness we have used theoretical, though approximate, expressions for processes (1) and (2) and have semiempirically fit these expressions to the data obtained when many different target thicknesses were used. The uncertainty in this correction is at least as large as the correction itself, which in no case was more than 12%. The final cross sections are listed in Table I together with the correction for finite target thickness and the total uncertainty.

### III. THEORY

#### A. Plane Wave Born Approximation

The electromagnetic interaction between a swift charged particle and an atomic electron can be subdivided into two terms:<sup>8-11</sup> the unretarded static Coulomb interaction and the interaction between the currents of the two particles. Both are responsible for the transfer of momentum from the projectile to the electron, causing K vacancy formation. The Coulomb interaction,  $Z_1 e^2 / |\vec{r} - \vec{r}_j|$ , where  $\vec{r}$  and  $\vec{r}_j$  are the position vectors of the projectile and electron respectively, can be written as a Fourier integral  $Z_1 e^2 / 2\pi^2 \int d\vec{k} k^{-2} \exp[i\vec{k} \cdot (\vec{r} - \vec{r}_j)]$ , where  $\vec{k}$  serves to transfer momentum from the projectile to the electron.

The current-current interaction may be viewed as the emission and reabsorption of a photon with momentum  $\hbar\vec{k}$ . Emission of a photon by the incident particle has a matrix element  $Z_1 e c \vec{\alpha} \cdot \hat{A}_S \exp(i\vec{k} \cdot \vec{r})$ , where  $\hat{A}_S$  is the photon's polarization vector and  $\vec{\alpha}$  is the current operator for the particle. Absorption by the electron is proportional to the matrix element of  $e c \vec{\alpha}_j \cdot \hat{A}_S \exp(i\vec{k} \cdot \vec{r}_j)$ . The implication of this view is that the current-current interaction may be evaluated equivalently in two ways: one can either proceed to evaluate these matrix elements by using the PWBA or we may use the completely classical Weizsäcker-Williams method of virtual photons. The Plane Wave Born method is discussed first.

Using the PWBA, the cross section for exciting an electron from state 0 to n while simultaneously producing a momentum loss in the projectile of  $\vec{q} = \vec{p} - \vec{p}'$  is given by<sup>11</sup>

$$d\sigma_n = \frac{m}{2\pi\hbar^4 v_1^2} |\langle \vec{p}'n | H_{\text{int}} | \vec{p} 0 \rangle|^2 q dq, \quad (3)$$

where  $v_1$  is the projectile velocity. From the preceding arguments the matrix element is given by

$$\begin{aligned} \langle \vec{p}'n | H_{\text{int}} | \vec{p} 0 \rangle &= \frac{Z_1 e^2}{2\pi^2} \times \int d\vec{k} \left\{ \langle \vec{p}' | \exp(i\vec{k} \cdot \vec{r}) | \vec{p} \rangle \langle n | \sum_j \exp(i\vec{k} \cdot \vec{r}_j) | 0 \rangle \right. \\ &+ \left. \sum_S \langle \vec{p}' | \alpha \cdot \hat{A}_S \exp(i\vec{k} \cdot \vec{r}) | \vec{p} \rangle \langle n | \sum_j \alpha_j \cdot \hat{A}_S \exp(i\vec{k} \cdot \vec{r}_j) | 0 \rangle \right\}, \quad (4) \\ &\frac{k^2 - (E_n/\hbar c)^2} \end{aligned}$$

where  $Z_1$  is the projectile charge,  $E_n$  ( $\equiv E_n - E_0$ ) is the energy of the excited state, and the sum  $\sum_S$  stands for the sum over intermediate states which have an emitted photon and either the electron or projectile in an excited or de-excited state. The matrix elements depend on the spin of the particle and other relativistic variables, and the square of the matrix element must be averaged over these quantities. For the moment we will neglect these complications, however, and the matrix elements may be reduced, using

$$\begin{aligned} \langle \vec{p}' | \exp(i\vec{k} \cdot \vec{r}) | \vec{p} \rangle &= (2\pi)^3 \delta(\vec{k} + (\vec{p}' - \vec{p})/\hbar), \\ \langle \vec{p}' | \alpha \cdot \hat{A}_S \exp(i\vec{k} \cdot \vec{r}) | \vec{p} \rangle &= \beta \cdot \hat{A}_S (2\pi)^3 \delta(\vec{k} + (\vec{p}' - \vec{p})/\hbar) \end{aligned} \quad (5)$$

Where  $\beta = \vec{v}_1/c$ .

The first term in Eq. (4) is the Coulomb interaction, which exerts a force parallel to  $\vec{q} = \vec{p} - \vec{p}'$  and is therefore called "longitudinal". The interaction through virtual photons is "transverse" because the photon fields are perpendicular to  $\vec{q}$ . Following Fano<sup>11</sup> and

Eq. (5) we find

$$d\sigma_n = \frac{4\pi Z_1^2 e^4}{v_1^2} \left\{ \frac{|F_n(q)|^2}{q^4} + \frac{|\vec{\beta}_t \cdot \vec{G}_n(q)|^2}{(q^2 - (E_n/c)^2)^2} \right\} q dq, \quad (6)$$

where  $\vec{\beta}_t = \vec{\beta} - (\vec{\beta} \cdot \hat{q}) \hat{q}$  is the component of  $\vec{\beta}$  perpendicular to  $\hat{q}$ , and

$$\begin{aligned} F_n(q) &= \sum_j \langle n | \exp(i\vec{q} \cdot \vec{r}_j) | 0 \rangle, \\ \vec{G}_n(q) &= \sum_j \langle n | \vec{\alpha}_j \exp(i\vec{q} \cdot \vec{r}_j) | 0 \rangle. \end{aligned} \quad (7)$$

No interference between the longitudinal and transverse excitations is present because atomic states of different parity are excited by the different interactions.

The evaluation of  $F_n(q)$  is well understood.<sup>4</sup> The evaluation of  $\vec{G}_n(q)$  has been done also. Where  $n$  is a continuum state,  $\vec{G}_n(q)$  can be recognized as the matrix element for the photoelectron absorption of high-energy photons. In the spirit of the evaluation of  $F_n(q)$ , nonrelativistic one-electron  $1s$  and continuum wavefunctions are used and we equate  $\vec{\alpha}_j$  with  $\vec{v}_j/c = (iE_n/\hbar c)\vec{r}_j$ . Fisher<sup>16</sup> has given

$$|\vec{G}_n(q)|^2 = \frac{E_n^2}{(\hbar c)^2} \frac{Z^6 \exp\{2Z/k \arctan[2Zk/(k^2 - Z^2 - q^2)]\}}{2^3 [(q^2 + Z^2 + k^2)^2 - 2q^2 k^2]^2 [1 - \exp(-2\pi Z/k)]}, \quad (8)$$

where  $k^2/2 = \epsilon$  is the continuum energy and  $Z$  is the target atomic charge (elsewhere  $Z_2$ ). To obtain the total  $K$  vacancy cross section we need only integrate  $q$  from  $q_{\min} = E_n/\hbar v = (U_K + \epsilon)/\hbar v$  to  $q_{\max} = |p| \approx \infty$  and over the continuum energy  $\epsilon$ . Introducing the variables  $x = \cos^2 \psi = q_{\min}^2/q^2$  and  $y = k^2/Z^2$ , we find the transverse excitation

cross section after a few manipulations:

$$\sigma_K^t = 1.6 \times 10^6 \beta^2 (Z_1^2/Z_2^2) g(\eta_K, \beta^2) \text{ (barns)},$$

where  $g(\eta_K, \beta^2)$  is a universal function given by

$$g(\eta_K, \beta^2) = \int_0^\infty dy (1+y)^{-1} \int_0^1 \frac{(1-x) dx}{(1-\beta^2 x)^2} \times \frac{\exp\{2/\sqrt{y} \arctan [2\sqrt{y}/(y-1-P)]\}}{[(P+1+y)^2 - 2yP]^2 [1-\exp(-2\pi/\sqrt{y})]}, \quad (10)$$

with  $P = (1+y)^2/4\eta_K$  and  $\eta_K = (v_1/v_K)^2$

We shall discuss the numerical evaluation of  $g(\eta_K, \beta^2)$  over a wide range of  $\beta^2$  and  $\eta_K$  in a later publication. Here, we shall concentrate our attention on the case in which  $\beta^2 \approx 1$ , where the integral over  $x$  is strongly peaked at  $x=1$ . We can approximate Eq. (10) by letting  $x=1$  for all but the peaking factor, reducing the double integral to two single integrals:

$$\begin{aligned} g(\eta_K, \beta^2) &\approx \int_0^1 \frac{(1-x) dx}{(1-\beta^2 x)^2} \int_0^\infty \frac{dy (1+y)^{-1} \times \exp\{2/\sqrt{y} \arctan [2\sqrt{y}/(y-1-P)]\}}{[(P+1+y)^2 - 2yP]^2 [1-\exp(-2\pi/\sqrt{y})]} \quad (11) \\ &= [\ln(\gamma^2) - \beta^2]/\beta^4 g'(\eta_K), \end{aligned}$$

when  $P$  is now  $(1+y)^2/4\eta_K$  and  $\gamma = [1-\beta^2]^{-1/2}$ . We have found numerically that  $g'(\eta_K)$  is a slowly varying function which changes from  $5.7 \times 10^{-3}$  for  $\eta_K = 1$  to  $6.6 \times 10^{-3}$  for  $\eta_K = \infty$ .

Finally, it may be shown that in the limits of  $q_{\min} \approx 0$  or  $\eta_K \approx \infty$ , one may evaluate  $G_n(q)$  by making the dipole approximation, i.e., setting  $\exp(i\vec{q} \cdot \vec{r}) = 1$ . The matrix element is then the same as that given by Bethe and Salpeter<sup>17</sup> and, following a similar analysis, we obtain  $g(\eta_K \approx \infty) = 6.6 \times 10^{-3}$ . Hence in the dipole approximation, the transverse cross section is given by

$$\sigma_K^t = 1.056 \times 10^4 \frac{z_1^2}{z_2^2} [\ln(\gamma^2) - \beta^2] / \beta^2 \text{ (barns)}. \quad (12)$$

### B. The Classical Evaluation

The form of the matrix element for the current-current interaction suggests that one may use the Weizsacker-Williams method of virtual photons.<sup>18,19</sup> We review this method in the following section.

The field of a projectile passing by an electron with an impact parameter  $b$  has a spectrum of virtual quanta given by the square of the Fourier transform of the time-dependent electric field:

$$\frac{dN(\omega, b)}{d(\hbar\omega)} = \frac{c}{2\pi(\hbar\omega)} |\vec{E}(\omega, b)|^2, \quad (13)$$

where

$$\vec{E}(\omega, b) = \int_{-\infty}^{\infty} dt \vec{E}(t) e^{i\omega t}$$

and the time integral is over a trajectory with a given projectile velocity and electron-projectile impact parameter. To obtain the total spectrum, we integrate over impact parameter:

$$\begin{aligned} \frac{dN(\omega)}{d(\hbar\omega)} &= \int_{b_{\min}} 2\pi b db \frac{dN(\omega, b)}{d(\hbar\omega)} \\ &= \frac{2}{\pi} \frac{z_1^2 e^2}{c^2 \omega \beta^2} \left\{ x K_0(x) K_1(x) - \frac{1}{2} \beta^2 x^2 [K_1^2(x) - K_0^2(x)] \right\}, \end{aligned} \quad (14)$$

where  $x = \frac{\omega b_{\min}}{\gamma v}$ ,  $\gamma = (1 - \beta^2)^{-1/2}$ , and  $K_n(x)$  are the usual modified Bessel functions. For  $x \ll 1$ , the spectrum can be approximated by:

$$\frac{dN}{d(\hbar\omega)} = \frac{2}{\pi} \frac{z_1^2 e^2}{c^2 \omega \beta^2} \left[ \ln \left( \frac{1.123 \gamma v}{\omega b_{\min}} \right) - \beta^2 / 2 \right]. \quad (15)$$

So far we have not specified  $b_{\min}$ . A non-zero choice of  $b_{\min}$  must be made in order to obtain a nondivergent spectrum. The choice usually made in these problems is to use the radius of electron shell from which excitation occurs, which in this case is the K shell radius  $a_K$ . The argument for this choice is that for impact parameters less than  $a_K$  the expansion of the interaction into multipoles fails and the dipole approximation can no longer be trusted. Other arguments have been given.<sup>20</sup> Unfortunately, the final results will not be insensitive to the choice of  $b_{\min}$ .

Photons of energy  $\hbar\omega_X > U_K$  can photoelectrically excite K electrons giving a net cross section

$$\sigma_K^{WW} = \int_{U_K}^{\omega_0} \sigma_{PE}(\omega_X) \frac{dN}{d\omega_X} d\omega_X, \quad (16)$$

where  $\omega_0$  is the cutoff frequency  $1.123 \gamma\beta c/a_K$ , and  $\sigma_{PE}$  is the photoelectric cross section per atom given by

$$\sigma_{PE} = \frac{84}{(\alpha^3 Z^2)} \left[ \frac{U_K}{\hbar\omega_X} \right]^4 \frac{\exp(-4n \cot^{-1}n)}{(1 - e^{-2\pi n})} \text{ (barns)} \quad (17)$$

with  $n = \left[ \hbar\omega_X/U_K - 1 \right]^{-1/2}$ . Following Kolbensvedt,<sup>21</sup> (16) is integrated (with approximations) and we find

$$\sigma_K^t = 1.056 \times 10^4 Z_1^2/Z_2^2 [\ln(2.4\eta_K \gamma^2) - \beta^2]/\beta^2 \text{ (barns)}. \quad (18)$$

Except for the factor  $\ln 2.4\eta_K$ , this is equivalent to the dipole - PWBA. In the range of  $\eta_K$  that we are interested in, this factor makes a large difference in  $\sigma_K^t$ , hence the Weizsäcker-Williams method will not be a good approximation.

One can possibly improve the classical calculations by introducing more sophisticated expressions for the virtual photon field<sup>22</sup> and by using fully retarded expressions for the photoelectric cross section. Such an approach, however, is liable to be more complicated than the PWBA method for which we already have results.

### C. The Total Cross Section

In using the classical method one generally adds to the Weizsäcker-Williams cross section the integrated cross section for the Rutherford scattering of the electron from the projectile with an energy transfer<sup>18</sup>  $\epsilon > U_K$  (valid for very large  $n_K$ ). At this point a discussion about the integral over impact parameters is generally made. The Weizsäcker-Williams cross section was integrated over impact parameters  $b > a_K$ , and is therefore a distant collision cross section. The Rutherford cross section, representing the interaction between the static Coulomb fields, is a close collision cross section. It is generally thought that one should be careful not to double-count impact parameters, i.e., one should just take the Rutherford cross section integrated from  $b = 0$  to  $a_K$ .<sup>18,19</sup>

We would like to emphasize that since the Weizsäcker-Williams and Rutherford cross sections come from two different interactions, they should both be integrated over all impact parameters, hence there should be no concern about double counting. The only reason why the Weizsäcker-Williams cross section was not integrated to  $b = 0$  was to obtain a nondivergent virtual photon cross section. This is just a peculiarity of the method. The total cross section is therefore given by summing

$$\sigma_K = \sigma_K^l + \sigma_K^t, \quad (19)$$



where  $\sigma_K^l$  can be either the PWBA, BEA, or SCA cross section for the Coulomb interaction and  $\sigma_K^t$  can be either the Weizsäcker-Williams or the PWBA cross section for the current-current interaction.

#### IV. DISCUSSION

In Fig. 3 we compare the experimental cross sections to two theoretical calculations. The classical calculation is obtained by adding the Weizsäcker-Williams cross section to the BEA cross section.<sup>1</sup> The BEA theory accounts for the Rutherford scattering of an electron of velocity  $\vec{v}_2$  by a projectile with velocity  $\vec{v}_1$  giving an energy transfer  $\epsilon$ . A formula like (2) is used except that an additional average over the direction of  $\vec{v}_1$  and  $\vec{v}_2$  and the initial electron speed  $v_2$  is done. For the PWBA cross sections, the longitudinal contribution is given by Khandewal et al.<sup>23</sup> The transverse contribution was obtained by numerically evaluating Eq.(10). Based on our earlier discussion, we believe the remarkable agreement between the classical calculation and experiment is fortuitous.

The transverse excitation contribution clearly brings the PWBA evaluation closer to experiment, though perfect agreement is still not obtained. It is curious that the deviations are more pronounced for the higher Z elements where  $n_K$  is smallest and indeed overlaps previous measurements. Whether this indicates the importance of a relativistic term in  $(\alpha Z)^n$  we cannot say.

It has been pointed out that the Bethe Approximation<sup>24,25</sup> agrees quite well with our experimental results. The Bethe Approximation incorporates the transverse as well as longitudinal contributions, but

is based on the dipole approximation to matrix elements of  $\exp(i\vec{q}\cdot\vec{r})$  and  $\vec{\alpha} \exp(i\vec{q}\cdot\vec{r})$ . The approximation predicts a ratio of experiment to theory of 1.4 for Ni and 1.0 for U which is considerably better than our evaluation. However, we question the validity of the dipole approximation in these cases where  $qa_K \sim [4\eta_K]^{-1/2}$  is of the order of 0.1-0.5 instead of 0. While for the transverse contribution the dipole approximation seems adequate (see Eq.(11)), it does not seem appropriate for the longitudinal contribution. Comparing Khandewal's<sup>23</sup> universal function  $f(\eta_K, \theta_K \sim 1)$  for the longitudinal cross section with the dipole approximation to it, we find serious disagreements for  $\eta_K \lesssim 5$  ( $Z_2 \gtrsim 60$  for 4.88 GeV protons). The fully retarded matrix element is smaller than the dipole approximation; hence, the better agreement for the heavy-Z, low  $\eta_K$  elements is fortuitous.

We have used the PWBA to calculate the transverse excitation contribution to systems other than 4.88-GeV protons. Basically, the contribution is negligible in all heavy-particle data that have ever been taken. For instance for 30-MeV p + Ti, the contribution only increases  $\sigma_K$  by  $3.3 \times 10^{-4}$ . The second highest velocity measurement was made with 160-MeV protons by Jarvis *et al.*<sup>7</sup> There, the contribution ranges from  $4.2 \times 10^{-3}$  for Ti to  $2.6 \times 10^{-3}$  for U. These results are not surprising, since in all of these cases, the projectile current has  $\beta^2 \ll 1$ . Hence, the current-current interaction is expected to be small.

Finally we show how the total PWBA cross section behaves at even higher energies. Since the longitudinal cross section depends only on the ratio of the projectile velocity to the K electron velocity, the higher energy behavior of this cross section is expected to be constant

for  $T \geq 5$  GeV. However, the transverse contribution rises like the  $\log \gamma^2$ , hence the total cross section also rises. Figure 4 shows the K cross sections for protons on Sn as a function of kinetic energy up to 10,000 GeV. It is interesting now to return to the point made by Jarvis et al.<sup>7</sup> By comparing proton-induced K excitation cross sections with relativistically calculated electron-induced K excitation cross sections, they had previously suggested the kind of rise that is shown in this curve. However, the reason the electron K excitation curve rises is because of the transverse term. In fact, the behavior of the longitudinal and transverse contributions in the electron theory<sup>21</sup> is qualitatively similar to that displayed in Fig. 4. The longitudinal part approaches a constant at high incident electron energies, while it is the transverse contribution that causes the cross section to rise.

## V. CONCLUSIONS

Cross sections for K vacancy production by 4.88-GeV protons were measured, and they disagreed significantly with the BEA and PWBA predictions. We argue that the BEA and PWBA theories of K vacancy production are correctly extended to relativistic energies when the correct velocity  $v_1 = \beta c$  is used in the scaling parameter  $(v_1/v_K)^2$ . Those theories only account for the interaction between the static Coulomb fields of the projectile and target electrons. Besides this, a contribution due to the interaction between the projectile and electron currents must be added to these cross sections.

The transverse interaction between charged particles and matter has previously been included in calculations of stopping powers<sup>11</sup> and K-vacancy production by incident electrons<sup>21</sup>. The reason why it has not been mentioned in connection with K-vacancy production by protons and heavy ions is because in all previous measurements of this kind the incident projectile velocity had  $\beta \ll 1$ , and the transverse term was entirely negligible. Many relativistic proton accelerators exist throughout the world and we hope that this experiment will inspire others to more fully examine the contribution of the transverse interaction to inner shell vacancy production.

## Acknowledgments

We are indebted to the operating staff of the BEVALAC for their great support. These experiments are one of the series of our TOSABE collaboration, the acronym denoting the three principal centers in Tokyo, Osaka, and Berkeley. We gratefully acknowledge the encouragement of Professors Sakai, Sugimoto, Nakai, Chamberlain and Steiner.

We acknowledge valuable comments on this work from E. Merzbacher, M. Inokuti, Y. K. Kim, J. Wu, J. McGuire, and J. D. Jackson.

This report was done with partial support from the United States Energy Research and Development Administration.

Footnote and References

\*Present address: Dept. of Physics, Stanford University, Stanford, CA 94305.

1. J. D. Garcia, R. J. Fortner, and T. M. Kavanagh, Rev. Mod. Phys. 45, 111 (1973).
2. J. D. Garcia, Phys. Rev. A 1, 280 (1970).
3. J. H. McGuire and P. Richard, Phys. Rev. A 8, 1374 (1973).
4. E. Merzbacher and H. Lewis, Encyclopedia of Physics (Springer-Verlag, Berlin, 1958), Vol. 34, p. 166.
5. J. Bang and J. M. Hansteen, K. Dan. Vidensk. Selsk. Mat.-Fys. Medd. 31, 13 (1959).
6. Measurements for 18-MeV proton+carbon ( $v_1/v_K=5.9$ ) were recently reported by D. Burch, Phys. Rev. A 12, 2225 (1975).
7. O. N. Jarvis, C. Whitehead, and M. Shah, Phys. Rev. A 5, 1198 (1972), and unpublished Harwell report AERE-R-6612 (1970).
8. C. Müller, Ann. Phys. (Leipz.) 14, 531 (1932).
9. H. Bethe, Z. Phys. 76, 293 (1932).
10. U. Fano, Phys. Rev. 102, 385 (1956).
11. U. Fano, Annu. Rev. Nucl. Sci. 13, 1 (1963).
12. J. B. Cummings, Annu. Rev. Nucl. Sci. 13, 260 (1963).
13. For more recent values of the  $^{11}\text{C}$  cross section we refer to A. Smith, LBL, private communication (1975).
14. W. H. McMaster, N. Kerr Del Grande, and J. H. Mallett, unpublished report UCRL-50174, Section II (1969).

15. W. Bambynek, B. Craseman, R. W. Fink, H.-U. Freund, H. Mark, C. D. Swift, R. E. Price, and P. Venugopula Rao, *Rev. Mod. Phys.* 44, 716 (1972).
16. J. Fischer, *Ann. Phys. (Leipz.)* 8, 821 (1931).
17. H. Bethe and E. E. Salpeter, *Encyclopedia of Physics* (Springer-Verlag, Berlin, 1957), Vol. 24, Sec. 71.
18. E. J. Williams, *K. Dan. Vidensk. Selsk. Mat.-Fys. Medd.* 13, 4 (1935).
19. J. D. Jackson, *Classical Electrodynamics* (Wiley, New York, 1962).
20. J. D. Jackson and R. L. McCarthy, *Phys. Rev. B* 6, 4131 (1972).
21. H. Kolbentsvedt, *J. Appl. Phys.* 38, 4785 (1967).
22. R. Jäckle and H. Pilkuhn, *Nucl. Phys. A* 247, 521 (1975).
23. G. S. Khandewal, B. H. Choi, and E. Merzbacher, *Atomic Data* 1, 103 (1969). The Ni point in Fig. 3 involves an extrapolation beyond the end of this table and is consequently uncertain.
24. M. Inokuti, *Rev. Mod. Physics* 43, 297 (1971).
25. Calculations made by Y.-K. Kim, M. Inokuti, E. Merzbacher, and J. Wu.

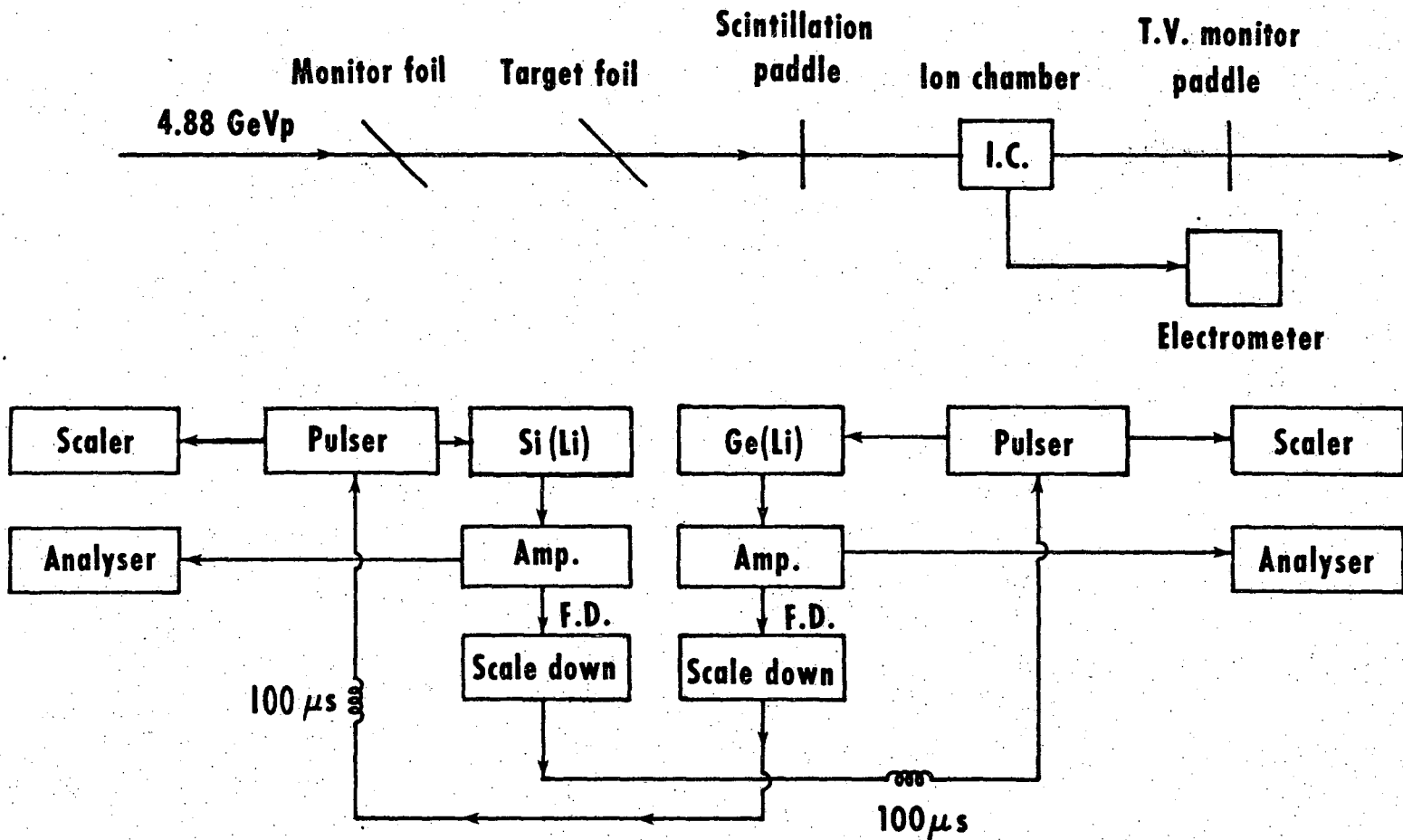
TABLE I. K vacancy cross sections from 4.88-GeV protons.

$Z_2$	$\sigma$ (barns)	Finite target thickness correction (%)
Ni	$210 \pm 25$	2.2
Zr	$102 \pm 12$	4.0
Mo	$94 \pm 12$	5.6
Ag	$58 \pm 10$	11.8
Tb	$31 \pm 7$	10.7
Ta	$22 \pm 4$	6.7
Pt	$18 \pm 4$	0.7
Au	$17 \pm 3$	2.8
Pb	$15 \pm 3$	2.7
U	$11 \pm 3$	1.9



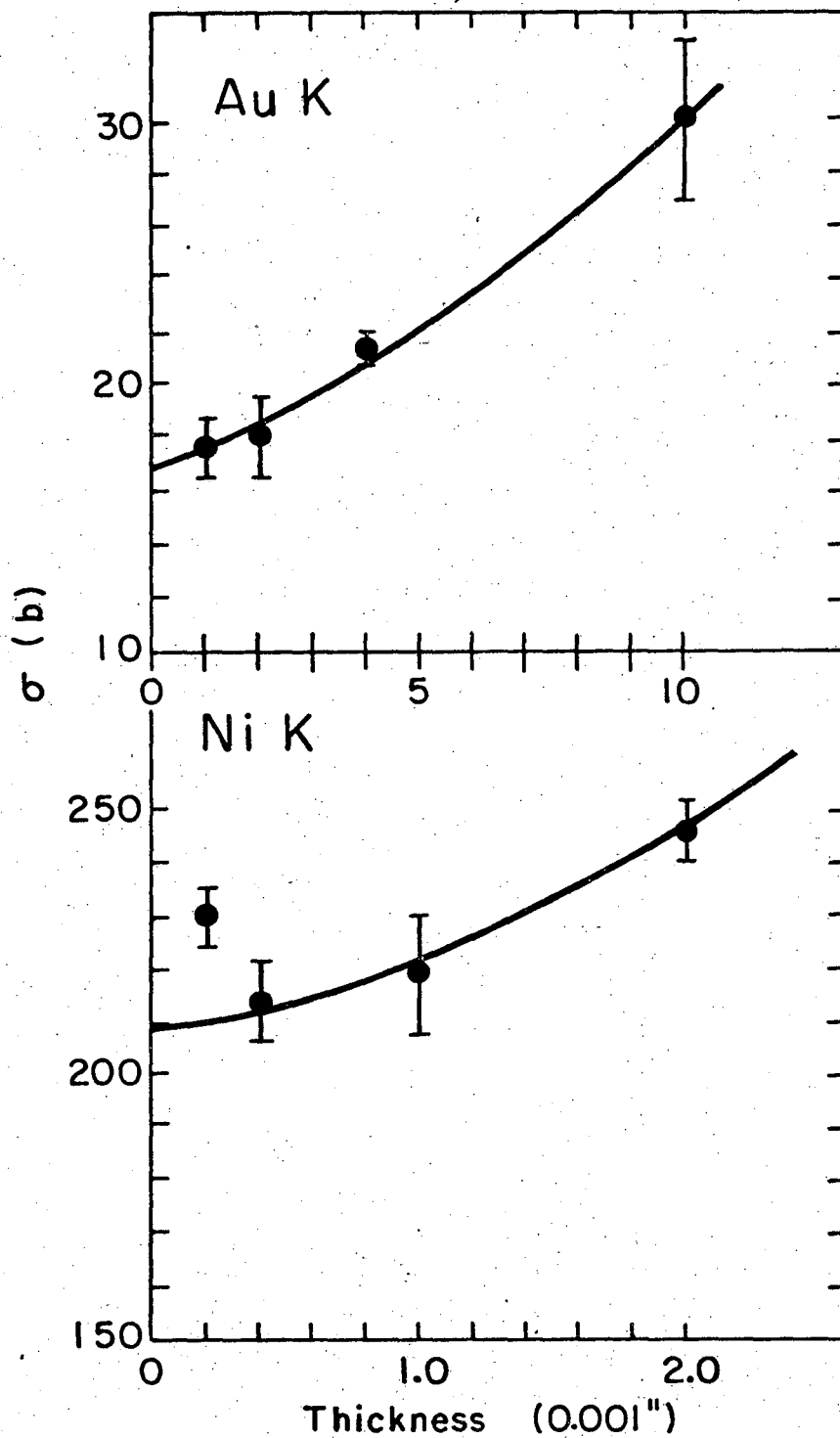
## Figure Captions

- Fig. 1. Schematic diagram showing experimental apparatus layout. FD: fast discriminator; Amp: amplifier, pileup rejector.
- Fig. 2. Experimental cross section versus target thickness. Error bars are relative error only. Curve gives approximation to quadratic thickness dependence.
- Fig. 3. Ratios of experimental cross sections for 4.88-GeV protons to theory. Lines are drawn to guide the eye only. Error bars are included for  $\sigma_{\text{exp}} / (\sigma_{\text{PWBA}}^{\ell} + \sigma_{\text{PWBA}}^{\text{t}})$  only.
- Fig. 4. Very high-energy behavior of p + Sn cross section calculated by using the PWBA.



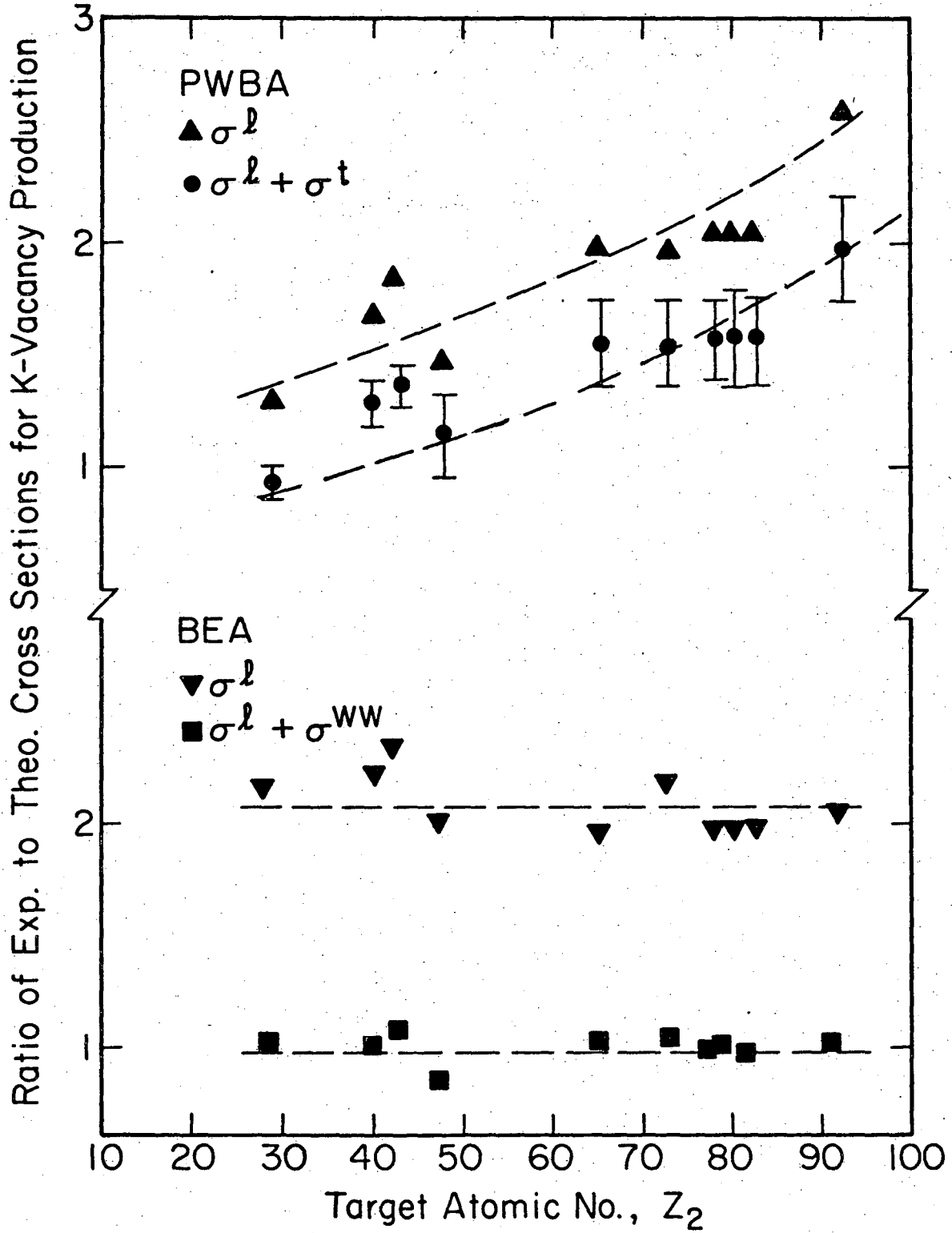
XBL759-3992

Fig. 1



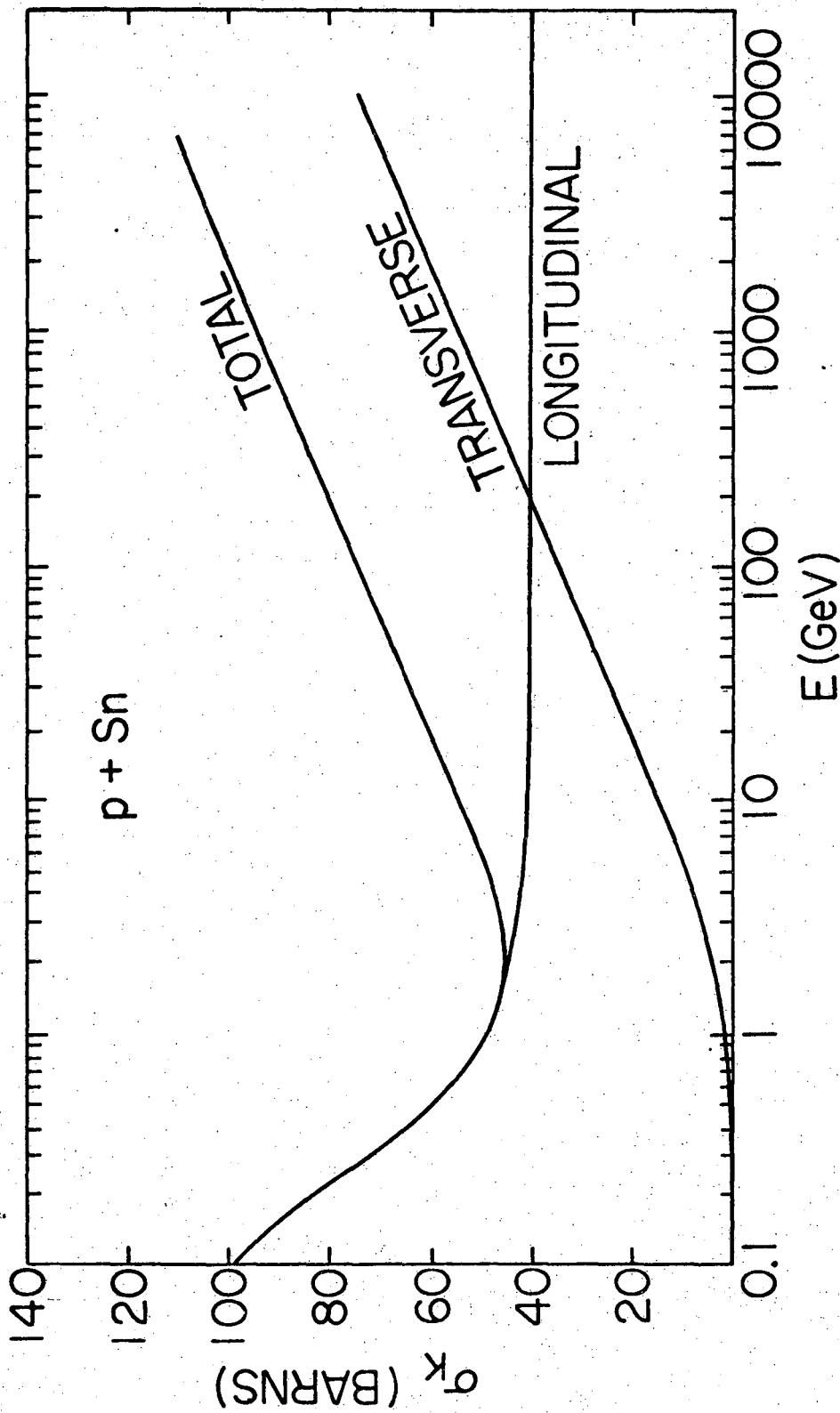
XBL759-3990

Fig. 2



XBL 764-1578

Fig. 3



XBL 766-8139

Fig. 4

**LEGAL NOTICE**

*This report was prepared as an account of work sponsored by the United States Government. Neither the United States nor the United States Energy Research and Development Administration, nor any of their employees, nor any of their contractors, subcontractors, or their employees, makes any warranty, express or implied, or assumes any legal liability or responsibility for the accuracy, completeness or usefulness of any information, apparatus, product or process disclosed, or represents that its use would not infringe privately owned rights.*

TECHNICAL INFORMATION DIVISION  
LAWRENCE BERKELEY LABORATORY  
UNIVERSITY OF CALIFORNIA  
BERKELEY, CALIFORNIA 94720